

# Performance assessment of geopolymer concrete with partial replacement of ferrochrome slag as coarse aggregate



Sanghamitra Jena, Ramakanta Panigrahi\*

Department of Civil Engineering, VSSUT, Burla 768018, Odisha, India

## HIGHLIGHTS

- Maximum strength of FSGPC is achieved at FS content 30%.
- Use of FS shows excellent performance in GPC as compared to NCA.
- Compact and denser media in the microstructure responsible for high strengths.

## ARTICLE INFO

### Article history:

Received 5 February 2019  
Received in revised form 2 June 2019  
Accepted 5 June 2019  
Available online 24 June 2019

### Keywords:

Geopolymer concrete  
Ferrochrome slag  
Compressive strength  
Split tensile strength  
Flexural strength

## ABSTRACT

The present research work aims to produce fly ash geopolymer concrete with ferrochrome slag as coarse aggregate. The experimental results of all the properties of ferrochrome slag based geopolymer concrete are compared to controlled geopolymer concrete and proved as most efficient, technically acceptable and environmentally compatible construction material. From compressive strength, flexural strength and split tensile test results, it is observed that ferrochrome slag based geopolymer concrete shows excellent performance than that of controlled geopolymer concrete. Further, scanning electron microscopy (SEM), Energy dispersive X-ray analysis (EDX), Fourier transformed infrared spectroscopy (FTIR) and X-ray diffraction (XRD) analyses are performed to study the behavior of microstructure with effect of different conditions.

© 2019 Elsevier Ltd. All rights reserved.

## 1. Introduction

In last three decades, different industrial wastes are widely used as coarse aggregate in concrete. Main ingredient is aggregate which has greater impact in the concrete as it occupies 75% of its volume. Aggregates directly affect the fresh and hardened properties [1]. Rapid growth of population and increased urbanization are the main factors to increase the demand of concrete. To reduce the demand of natural resources and environmental pollution, industrial wastes were used. Major CO<sub>2</sub> production occurs during manufacturing of cement. Annually, production quantity increases 3%. Nearly about 0.94 tons of CO<sub>2</sub> releases from the manufacturing of tones cement. SO<sub>3</sub>, NO<sub>x</sub> are greenhouse gases which are also released from cement industry. To maintain the ecological balance, the researchers develop sustainable construction material i.e.

geopolymer concrete as an alternative to replace cement concrete. Geopolymer concrete (GPC) is an innovative construction material which reduces the demand of ordinary Portland cement (OPC), preserve the natural resources, achieve the environmental safety, solves the disposal problems of industrial wastes and also produces high strength concrete [2]. In recent past, preparation of sustainable concrete using wastes and industrial byproducts has drawn attention of researchers. Geopolymer concrete is the interesting innovation of various researchers as a real substitute of Portland cement concrete. Ferrochrome slag is a solid waste material generated from the ferro alloy manufacturing industries. This slag has excellent potentiality to perform engineering and mechanical properties when used as coarse aggregate.

This research work emphasizes on the utilization of ferrochrome slag (FeCr) as coarse aggregate in GPC. Ferrochrome slag (FS) is the waste product that generates from stainless steel manufacturing industry. This slag is formed at a temperature more than 1600 °C as liquid. In India, nearly about 3.36 MT of FS are produced from 118 plants among operating total 229 furnaces [3]. The high production FS causes a serious disposal problem and affects the

Abbreviations: GPC, geopolymer concrete; FS, ferrochrome slag; CS, compressive strength; STS, split tensile strength; SH, sodium hydroxide; SS, sodium silicate.

\* Corresponding author.

E-mail address: [rosy.sibun@gmail.com](mailto:rosy.sibun@gmail.com) (R. Panigrahi).

environment. Its mineralogical composition and mechanical properties indicate that FS has excellent potentiality to be used as coarse aggregate in concrete [4]. It was observed that FS can be used as coarse aggregate instead of natural aggregate which improves split tensile strength as well as flexural strength about 6–8% in concrete [1]. Alternative cementing materials which can fully replace the cement is geocement [5–7]. Geopolymer binder is the cement produced from the synthesis of aluminosilicate material and alkaline solutions or phosphoric acid solution [8]. Aluminosilicate materials such as fly ash, ground granulated blast furnace slag and metakaolin etc. reacted with sodium or potassium based highly alkaline solutions. Mechanical and durability properties of fly ash GPC was studied by different researchers [8–11]. Compressive strength of FS based concrete 1.5 times than that of controlled concrete [12]. To reduce landfill waste and use of natural resources, recycled aggregate was used as coarse aggregate in concrete. Many researchers studied the properties of concrete using recycled coarse aggregate [13–17].

The properties of pervious GPC using recycled aggregate was studied in which crushed concrete member and crushed clay bricks were used as two types recycled aggregate. Acceptable strengths were observed using this aggregate as compared to GPC with natural coarse aggregate [18]. Light weight GPC with recycled light weight block was proved as an excellent construction material for wall and partition wall [19].

It was revealed from literature that geopolymers proved as an alternative substitute material not only in case of strength in concrete but also in soil stabilization. Alkali activated fly ash was used to enhance the properties of soil stabilization [20]. Different properties of GPC made up of recycled fly ash slag from Integrated Gasification Combined Cycle were studied. It was reported that the fly ash activated with combination of SS and SH gives higher strength than that of activated with only SH activator solution [21]. Geopolymers has another advantage to remove heavy metals from waste water. Geopolymer composites made up of metakaolin powder mixed with sodium alginate solution and chitosan were used for the removal of lead (Pb) from waste water (Yan et al. 2019) [22]. GPC prepared with Ground granulated blast furnace slag and Rice husk ash (RHA) had better CS than that of GPC without RHA [23]. Physical and mechanical properties of fly ash and slag GPC with different types of micro-encapsulated phase change materials (MPCM) were studied. It was found that CS of GPC is more than that of OPC concrete but it reduces when MPCM was introduced to GPC [24]. Different geopolymerization behaviour was studied by taking ferrochrome slag and fly ash blends. It was observed that the blended fly ash and ferrochrome slag shows better results than the individual [25]. Mechanical properties were observed in the geopolymer mortar in which ferrochrome slag as binder. Strength was decreased with increasing water to binder ratio [26]. Ferrochrome slag was also used as fine aggregate and proved as suitable construction material for the preparation of concrete [27]. Optimum strength was achieved at 75% of steel slag as coarse aggregate in concrete [28].

## 2. Research significance

Many researchers have carried out their research work on geopolymer concrete, mortar and paste with FS as binder. However, FS as coarse aggregate in GPC has not been reported in literature till date. To fill the gap, the present study investigates the physical and mechanical properties of GPC using FS as partial replacement of coarse aggregate. Further, microstructures and mineralogical phases are studied through SEM and XRD analysis respectively. FTIR analysis is also conducted to study vibration

characteristics of ferrochrome slag based geopolymer concrete (FSGPC).

## 3. Experimental method

### 3.1. Materials

Fly ash was collected from HINDALCO, Sambalpur, Odisha. Specific gravity of fly ash was found to be 2.46 as per IS: 3812 (part-1) [29]. Locally available river sand was used as fine aggregate and its zone was III as per IS: 383 [30]. Two types of coarse aggregate material such as a) Natural coarse aggregate (NCA) b) FS were used as coarse aggregate as per IS: 383 [30]. Ferrochrome slag was collected from Indian Metals & Ferro Alloys Limited (IMFA). Alkaline activators such as SH and SS were used to activate the source material (fly ash) [31]. Commercially available SS with 98% purity ( $\text{SiO}_2 = 34.8\%$ ,  $\text{Na}_2\text{O} = 15.8\%$ ,  $\text{H}_2\text{O} = 47.5\%$ ) was used. Sieve analysis of natural coarse and fine aggregate was found as per IS: 2386 (part-1) [32]. Specific gravity, bulk density, water absorption, impact value, abrasion value, flakiness index and crushing value of NCA and FS was determined according to IS: 2386 (part-3) and IS: 2386 (part-4) [33,34]. Figs. 1 and 2 show the scanning electron microscopy (SEM) and Energy Dispersive X-Ray Analysis (EDX) of fly ash respectively. It was observed that from the SEM image, the fly ash particles are spherical in shape and random sizes. Surface of the particles are smooth. Fig. 2 shows the elemental compositions of fly ash. Figs. 3 and 4 shows the image of NCA and FS respectively. It was noticed that Si content was relatively high as comparison to other elements available. Chemical compositions of fly ash and ferrochrome slag are given in Table 1 obtained by X-ray fluorescence (XRF) analysis. Physical properties of aggregates are shown in Table 2.

### 3.2. Mixing, casting and curing

14 M SH solution was prepared by dissolving ( $14 \times 40$ ) 560 g of SH pellets in one litre of water. Molecular weight of SH is 40gm. SS to SH ratio was 2.5 and water to binder ratio was kept constant 0.17. Alkaline solution to binder ratio was 0.5. The solution was kept for 24 h to cool the heat produced during the exothermic reaction developed in sodium hydroxide and water molecules [35]. Compressive strength (CS) of  $100 \times 100 \times 100$  mm size concrete cubes was measured according to Indian standard code of practice in compression testing machine (2000 kN capacity). CS test results were collected after 7, 14 and 28 days respectively. Cylindrical

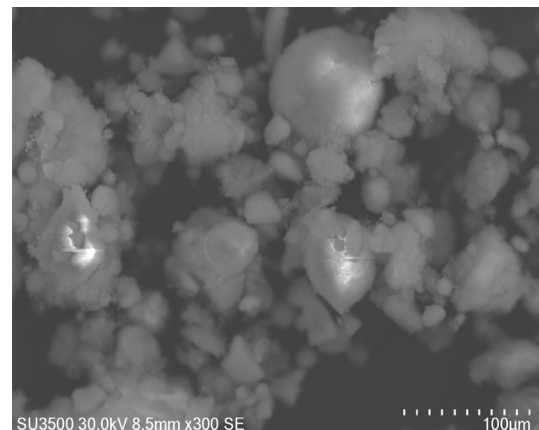


Fig. 1. SEM image of Fly ash.

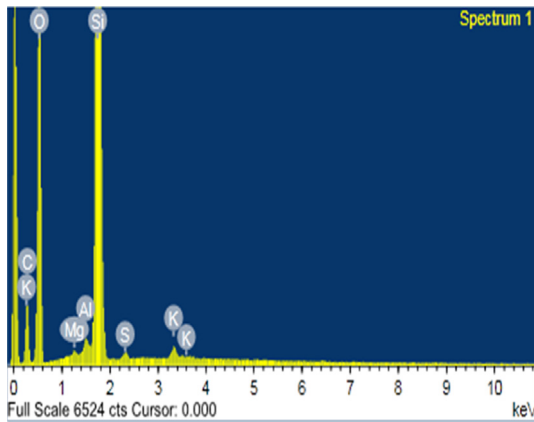


Fig. 2. EDX analysis of Fly ash.



Fig. 3. Image of natural coarse aggregate.



Fig. 4. Image of Ferrochrome slag aggregate.

specimens of  $150 \times 300$  mm size were tested after 28 days for split tensile strength in a 2000 kN capacity CS testing machine according to IS: 5816 [36]. Flexural strength test of  $100 \times 100 \times 500$  mm prisms were determined by Universal testing machine of 1000 kN capacity in accordance to IS: 516 [37].

All the aggregates were in saturated surface dry (SSD) condition. SS was added to the SH solution prior to the mixing of dry ingredients. Then proper mixing was done to produce concrete mix. Then the alkaline solution was added to the dry mix. Some amount of water was added only to increase the workability of the mix. Casting was done after the proper mixing. After casting the moulds were kept in the room temperature for 48 h for its setting. The moulds were demoulded and cured in the oven at  $70^\circ\text{C}$  for 24 h [31,38,39]. All the specimens were removed from the oven and kept at ambient temperature until the day of testing. Water absorption and density of 100 mm concrete cubes were found according to ASTM C 642–13 [40]. For each test, three specimens were tested and average of three results was reported in tables and figures. The mix proportions of GPC mix are shown in Table 3.

## 4. Result and discussion

### 4.1. Workability

Slump values of different GPC mixes with different percentage of ferrochrome slag as partial replacement of natural coarse aggregate is shown in Fig. 5. From Fig. 5, slump values of the GPC mixes 0%, 5%, 10%, 15%, 20%, 25%, 30%, 35% and 40% are found to be 61, 67, 75, 86, 94, 107, 113, 124 and 131 respectively. It is observed that the slump values were increased as the FS percentage increased. The reason for increasing slump value could be due to the higher water absorption capacity of FS than NCA. This experiment result is consistent with the study of previous researchers [4,41,42].

Fig. 6 shows the variation of slump value with geopolymer mixes prepared with different alkaline solution to binder ratio. The slump values for different solution to binder ratio i.e. 0.35, 0.4, 0.45, 0.5, 0.55, 0.6, 0.65 and 0.7 are found to be 85, 92, 101, 107, 115, 126, 132 and 145 respectively. It may be noted that slump values increases with increase in solution to binder ratio. Increasing solution to binder ratio was responsible for increasing Si content because sodium silicate solution content more Si species [43].

### 4.2. Compressive strength

Compressive strength of FSGPC at 7, 14 and 28 days is shown in Fig. 7. The 7, 14, 28 days CS of GPC mix without FS (control mix-FS0) were reported as 27.1 MPa, 31.3 MPa and 39.2 MPa respectively [44]. It was observed from Fig. 7 that CS of FSGPC increases up to 30% replacement of NCA with FS. Further increased FS percentage beyond 30% decreases the CS. The CS of geopolymer mix with 5%, 10%, 15%, 20%, 25% and 30% FS at 7 days increased from 27.1 MPa to 28.5 MPa, 29.5, 31.4, 32.5, 33.6, 34.1 and 36.2 MPa respectively. Maximum strength was achieved at 30% replacement with FS. CS decreased with further increase in percentage i.e. 35% and 40% of FS in geopolymer mix. Similar trends were observed at 30% substitution with FS at 14 days and 28 days. Increased percentage of FS increases the quantities of magnesium oxide and chromium. The activation of alkaline activators with MgO accelerates the early age strength. However, further increment causes leaching of chromium in the samples and with the activation of MgO produces hydrotalcite.

Fig. 8 shows the CS variation corresponding to different ratio of alkaline solution to binder. Eight different mixes G1-G8 were casted and cured with varying ratio of alkaline solution to binder. Ratio varies from 0.35 to 0.7 with regular interval of 0.05. It is noticed from the results that strength is increased from 0.35 to 0.6 rapidly, but significant decrease in strength is observed after 0.6 up to 0.7. This could be due to the increase of solution resulting the geopolymerization reaction more rapid which ultimately

**Table 1**  
Chemical compositions of Fly ash and FS were obtained by XRF.

Contents	SiO <sub>2</sub>	Al <sub>2</sub> O <sub>3</sub>	Fe <sub>2</sub> O <sub>3</sub>	CaO	MgO	Na <sub>2</sub> O	K <sub>2</sub> O	Cr <sub>2</sub> O <sub>3</sub>	SO <sub>3</sub>	P <sub>2</sub> O <sub>5</sub>	MnO
Fly ash	53.5	21.7	6.9	3.42	0.82	0.24	0.7	–	1.1	0.015	0.12
FS	27.8	23.6	3.6	3.51	23.7	0.21	0.15	9.16	–	–	–

**Table 2**  
Properties of coarse and fine aggregate.

Properties	Natural Fine aggregate	Natural Coarse aggregate	Ferrochrome slag	Max. limit
Specific gravity	2.76	2.87	2.63	2.5–3 (IS: 2386, P-3) [33]
Water absorption (%)	0.8	0.5	1.12	0.1–2 (IS: 2386, P-3)
Bulk density (loose) (kg/m <sup>3</sup> )	1460	1445	1480	–
Bulk density (Compact) (kg/m <sup>3</sup> )	1570	1578	1610	–
Impact value (%)	–	15.1	18.25	45 (IS: 383) [30]
Crushing value (%)	–	20.6	22.53	45 (IS: 383)
Abrasion value (%)	–	18.2	21.83	50 (IS: 383)
Flakiness index (%)	–	18.3	14.31	30 (IS: 383)

**Table 3**  
Mix proportion of FS based GPC.

GPC Mix	FA (kg/m <sup>3</sup> )	Sand (kg/m <sup>3</sup> )	NCA (kg/m <sup>3</sup> )	FS (kg/m <sup>3</sup> )	Alkaline (kg/m <sup>3</sup> )	SS (kg/m <sup>3</sup> )	SH (kg/m <sup>3</sup> )	Water (kg/m <sup>3</sup> )	Solution/binder ratio	Slump
FS0	410	590	1100	–	205	147	58	69	0.5	61
FS5	410	590	1045	55	205	147	58	69	0.5	67
FS10	410	590	990	110	205	147	58	69	0.5	75
FS15	410	590	935	165	205	147	58	69	0.5	86
FS20	410	590	880	220	205	147	58	69	0.5	94
FS25	410	590	825	275	205	147	58	69	0.5	107
FS30	410	590	770	330	205	147	58	69	0.5	113
FS35	410	590	715	385	205	147	58	69	0.5	124
FS40	410	590	660	440	205	147	58	69	0.5	131
G1	410	590	770	330	143.5	102.5	41	69	0.35	85
G2	410	590	770	330	164	117	47	69	0.4	92
G3	410	590	770	330	184.5	131.5	53	69	0.45	101
G4	410	590	770	330	205	147	58	69	0.5	107
G5	410	590	770	330	225.5	157	63	69	0.55	110
G6	410	590	770	330	246	176	70	69	0.6	126
G7	410	590	770	330	266.5	190.5	76	69	0.65	132
G8	410	590	770	330	287	205.5	82	69	0.7	145

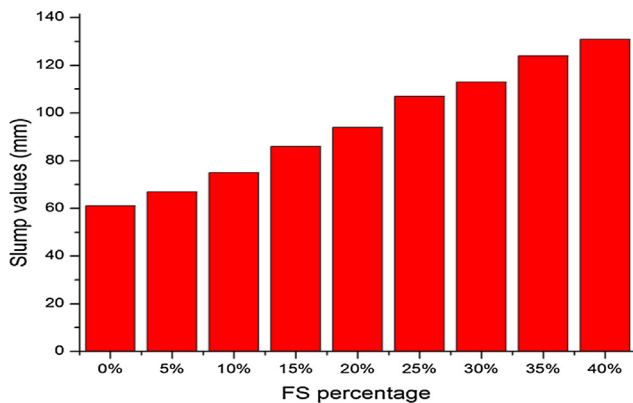


**Fig. 5.** Variation of slump values with FS percentage.

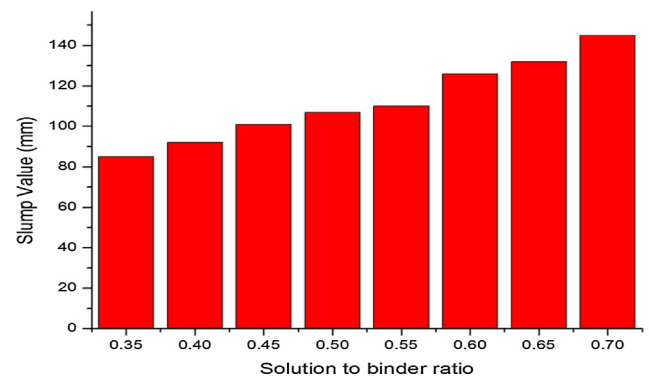


**Fig. 6.** Slump values with solution to binder ratio.

increases the strength. But at 0.65 and 0.7, solution contains more sodium silicate solution which increases the Si content [45]. This causes the more precipitation of Si species, which may be the reason of strength reduction after 0.6.

#### 4.3. Split tensile strength

After oven curing, GPC cylinders were tested with Universal testing machine. Nine GPC mixes were prepared with varying per-

centage of FS 0% to 40%. The results of split tensile strength (STS) are shown in Fig. 9. The 28 days STS of GPC was increased with the increase in percentage from 0 to 30% and significant decrease was noticed with varying percentage of FS from 35 to 40%. However, the tensile strength of FS35 and FS40 is found to be more than that of the controlled concrete (FS0). Optimum STS correspond to FS30 sample. Strength was achieved due to the geopolymerization reaction of Al–Si with alkaline activators [46]. FS has more density as well as strong than NCA. As the aggregate occupies more space in the concrete, it provides the strength. From the results, it is con-

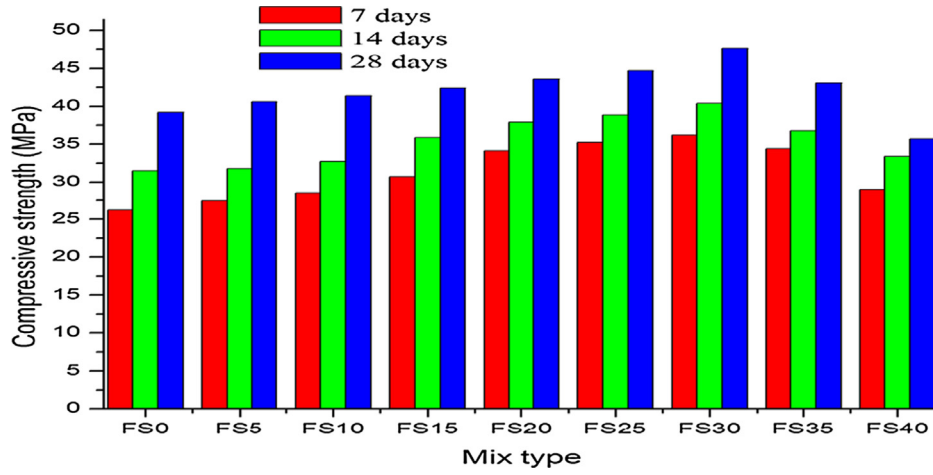


Fig. 7. Variation in compressive strength with varying percentage of FS.

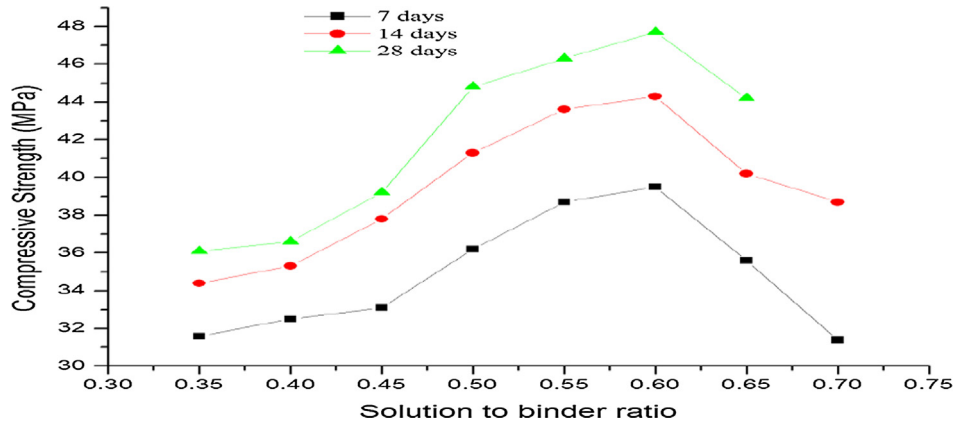


Fig. 8. Variation in compressive strength with varying solution to binder ratio.

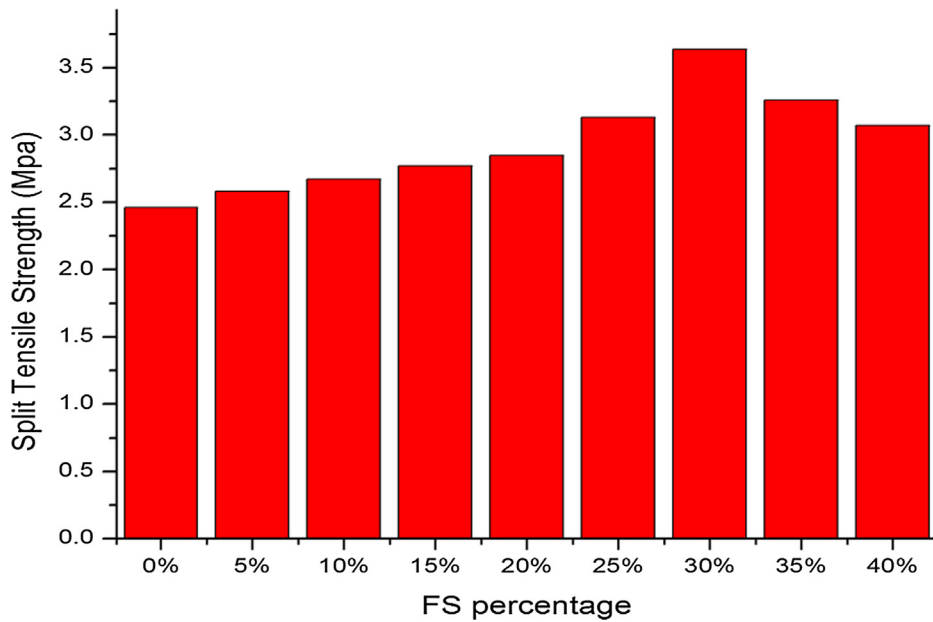


Fig. 9. Variation in split tensile strength with varying percentage of FS.

cluded that the STS increases with age. It is observed that the water absorption capacity of FS is more. At constant water to binder ratio, the amount of water absorption of FS is increasing with increasing percentage of FS. These mixes also absorbed more solution and that much of solution could not produce consistent mix. This could be the reason behind strength reduction. This mix was taken as reference mix for finding correlation between CS and STS. The ranges of CS at 7, 14 and 28 days are found as 36.3, 40.5 and 47.4 MPa respectively. The corresponding STS at 7, 14 and 28 days are 2.54, 3.16 and 3.64 MPa respectively.

Empirical formulae to establish the relationship between CS and STS in the form of equations were reported as given below [47,48].

$$\text{CEB - FIP : } f_{sp} = 0.301(f'_c)^{0.67} \tag{1}$$

$$\text{ACI363R - 92 : } f_{sp} = 0.59(f'_c)^{0.5} \tag{2}$$

$$\text{Gardener et al. : } f_{sp} = 0.6(f'_c)^{0.67} \tag{3}$$

$$\text{Ryu et al. : } f_{sp} = 0.17(f'_c)^{0.75} \tag{4}$$

where  $f_{sp}$  = Split tensile strength (MPa); and  $f'_c$  = Compressive strength (MPa).

Eqs. (1) and (2) were proposed by many researchers to find the relationship between CS and STS. Other researchers were established more relationship by providing the Eqs. (3) and (4) with the reference of the above mentioned basic equations [49,50].

Fig. 10 shows the relationship between CS and STS based on the several formulae established by ACI363R-92, CEB-FIP and other researchers. Fig. 10 shows that STS of the GPC with FS is lower than that proposed by CEB-FIP, ACI363R-92 and Gardener et al. However, experimental relation curve follows the similar trends to the model provided by the Ryu et al. [50] with marginal deviation. The deviation could be due to the higher CS of this model. Eq. (5) is

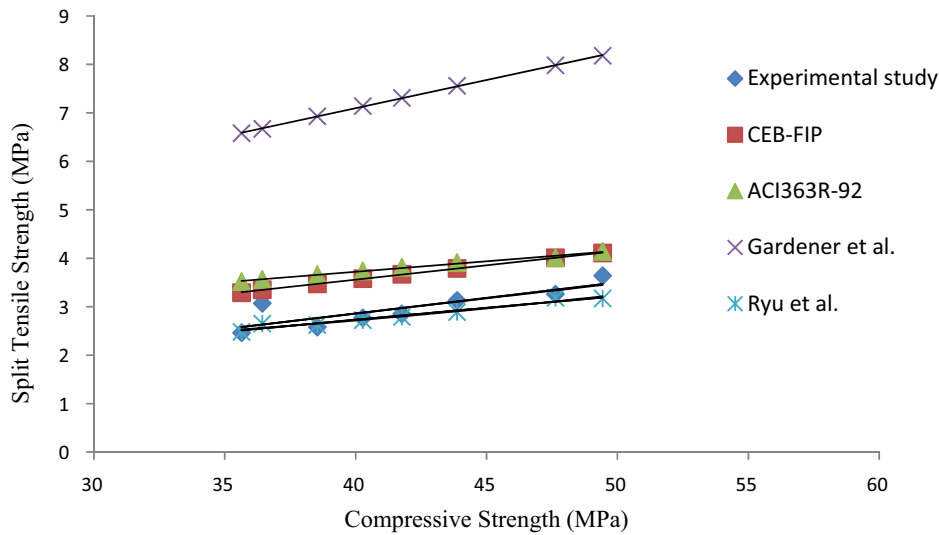


Fig. 10. Relation between CS and STS.

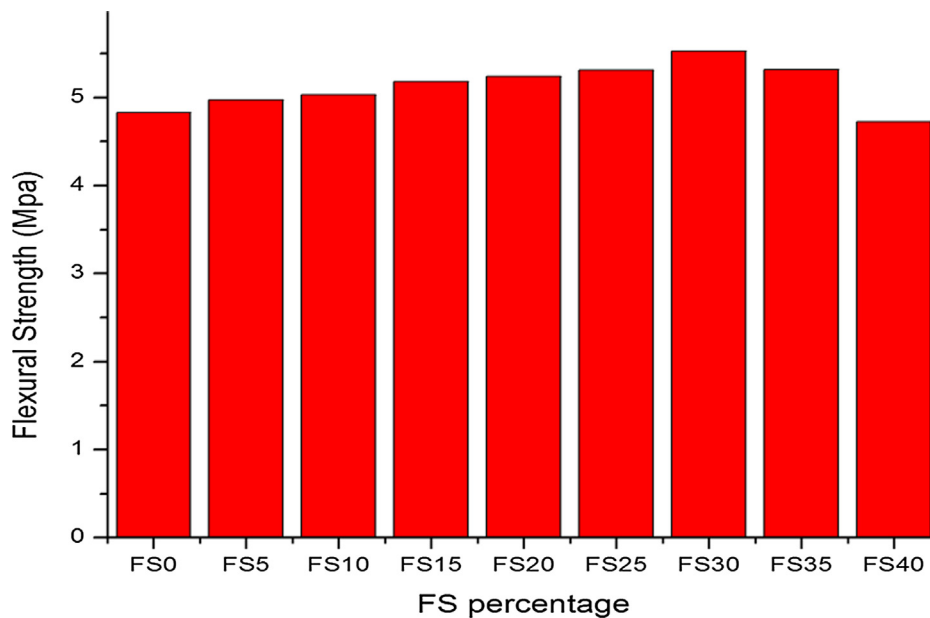


Fig. 11. Variation of flexural strength with different percentage of FS.

proposed as the correlation between experimental results obtained for STS and CS of FSGPC with FS content 30% of 14 M NaOH concentration combined with sodium silicate concentration at 70 °C for 24 h. The split tensile strengths of FSGPC in this study were related to the compressive strengths in Eq. (5) with  $R^2$  equal to 0.71.

$$f_{sp} = 0.11(f'_c)^{0.89} \tag{5}$$

#### 4.4. Flexural strength

The flexural strength at 28 days of fly ash GPC with varying percentage of FS is represented in Fig. 11. Nine separate mixes such as FS0, FS5, FS10, FS15, FS20, FS25, FS30, FS35 and FS40 were tested to find the flexural strength of each sample. The number represents the FS content in the GPC mix in percentage. Fig. 11 follows the similar trends as observed in STS. The mixes exhibit better resistant against flexural behaviour. In comparison to controlled GPC, the development of flexural strength is observed in increasing trend as FS content increases from 0 to 30%. Maximum strength is found in FS30 i.e. 5.83 MPa. Increase in FS content in GPC ultimately lead in increase of chromium content in the mix. The strength was decreased in FS 35 and FS40 mixes about 4% and 14% than that of FS30 respectively. FS35 mix has flexural strength

9% higher than the controlled mix (FS0). But FS40 mix has 2.5% lower strength than the controlled mix.

Fig. 12 shows the CS versus flexural strength of FSGPC. Flexural strength test result shows better performance than ACI 318-08 [51] and Sofi et al. [52]. This experimental study follows the similar trend line as proposed by Albitar et al. [31]. Strengths compared with the predicted models developed with the following Equations.

$$\text{ACI 318 - 08 (2008)} : "f'_{cf} = 0.62(f'_c)^{0.5}" \tag{6}$$

$$\text{Sofi et al.} : "f'_{cf} = 0.60(f'_c)^{0.5}" \tag{7}$$

$$\text{Albitar et al.} : "f'_{cf} = 0.75(f'_c)^{0.5}" \tag{8}$$

where  $f'_{cf}$  = Flexural strength (MPa); and  $f'_c$  = Compressive strength (MPa).

Regression analysis was done to find the relation between CS and flexural strength of FSGPC in terms of CS and is proposed in Eq. (9). The flexural strengths of FSGPC in this study were related to the compressive strengths in Eq. (9) with  $R^2$  equal to 0.84.

$$f'_{cf} = 0.78(f'_c)^{0.5} \tag{9}$$

#### 4.5. FTIR analysis

FTIR analysis was carried out by taking different samples of geopolymer mixes FS0, FS10, FS20 and FS30. The infrared spectra (IR) were found which covers 4000–400  $\text{cm}^{-1}$  range. The assignments of the IR spectra vibration bands of the samples were done by referring the previous materials and methods based on fundamental frequency of the vibrations of the Standard mineral data and reports of different researchers.

Fig. 13 shows the IR spectra of geopolymer mix with 0%, 10%, 20% and 30% FS respectively. After 28 days, sample of the specimen was taken for the FTIR analysis characteristics of IR spectra were assigned to vibrational bands. Fig. 13 shows weak absorption bands 3620  $\text{cm}^{-1}$ , 3653  $\text{cm}^{-1}$ , 3695  $\text{cm}^{-1}$  were assigned to Al–O–H stretching inner hydroxyl groups lying between tetrahedral and octahedral sheets. For the sample FS10, 960–1100  $\text{cm}^{-1}$  was

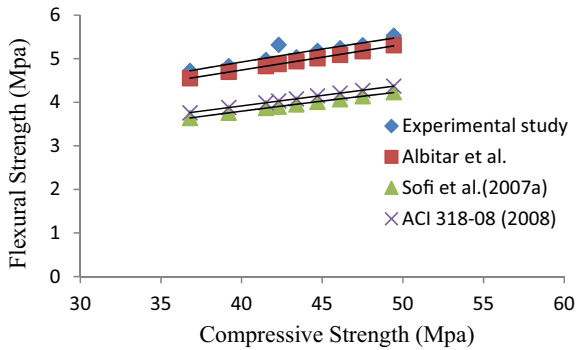


Fig. 12. Relation between CS and Flexural Strength.

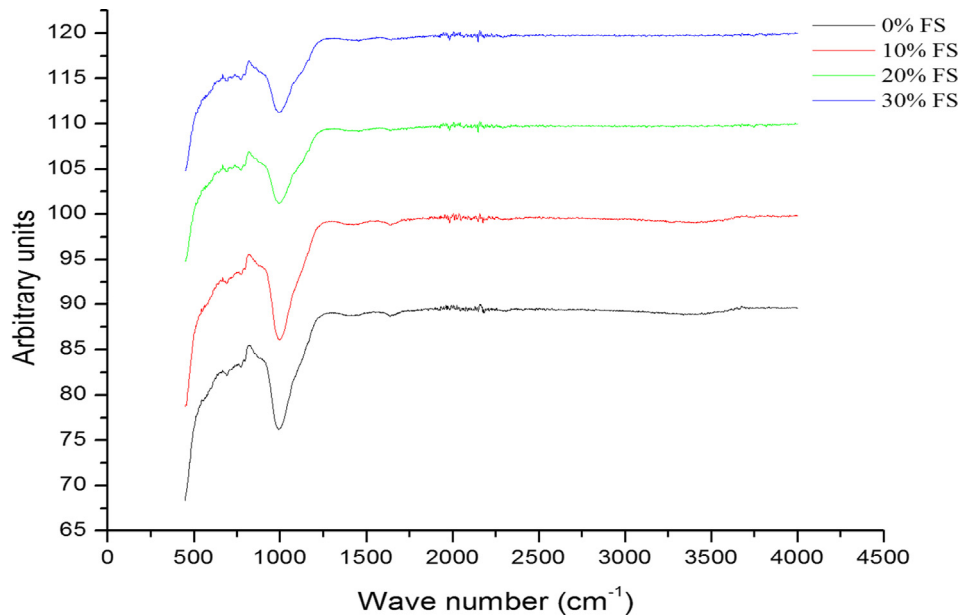


Fig. 13. IR spectra of Geopolymer mix.

assigned to strongest vibration of asymmetrical Si–O stretch. The band  $688\text{ cm}^{-1}$  may be attributed to stretching vibrations of Si–O–Si bond. This band was noticed when the ferrochrome slag was added to the FA GPC. Si–OH bending vibrations were assigned to  $850\text{ cm}^{-1}$ . Si–O–Al asymmetric stretch was assigned to  $974\text{ cm}^{-1}$  and  $1084\text{ cm}^{-1}$  region was assigned to Si–O–Si stretch. A strong H–O–H bending vibration was assigned to  $1600\text{ cm}^{-1}$  [53]. This could be due to the structural and entrapped air [25]. A strong absorbance was noticed at band  $999.2\text{ cm}^{-1}$  corresponding to 89.3% transmittance. A weak stretching vibration of –OH groups was noticed to  $3640\text{ cm}^{-1}$  region. Stretching vibration of Si–O of quartz may be attributed to the band  $691\text{ cm}^{-1}$ . Absorption was found at  $691.8\text{ cm}^{-1}$  with 93.77% transmittance.

The characteristic IR absorption bands and their vibrational assignments were used to determine the mineral constituents as well as temper of the samples. For the sample FS20, A weak stretch C–C triple bond was assigned to  $2149\text{ cm}^{-1}$ . This bond of alkynes

was weak in nature. The band  $1075\text{ cm}^{-1}$  may be attributed to the Al–Si–O stretching vibrations of amorphous aluminosilicates. Very weak H–O–H bending vibrations were assigned to  $1628\text{ cm}^{-1}$  of adsorbed water. Also  $3420\text{ cm}^{-1}$  band was assigned to weak stretching vibration of –OH group of adsorbed water molecules. Very weak bands  $3620\text{ cm}^{-1}$ ,  $3650\text{ cm}^{-1}$  were attributed to inner and external hydroxyl groups. Between tetrahedral and octahedral sheets, the inner hydroxyl group lies, this gives the strong absorption near  $3620\text{ cm}^{-1}$ . In this sample, maximum absorption was noticed at  $991\text{ cm}^{-1}$  band corresponding to 91.22% transmittance. This band was assigned to asymmetric stretching vibration of Si–O–Al and Si–O–Si band. This could be due to presence of FS [54,55]. Also of Si–O–Si bond was assigned to  $691\text{ cm}^{-1}$  band. Another two bands  $694.3\text{ cm}^{-1}$  and  $773.5\text{ cm}^{-1}$  moderately absorbed w. r. t 94.7% and 94.84% transmittance respectively.

Sample FS30 shows a strong vibration band  $999\text{ cm}^{-1}$  corresponds to the asymmetric stretching of Si–O–Si and Al–O–Si bond.

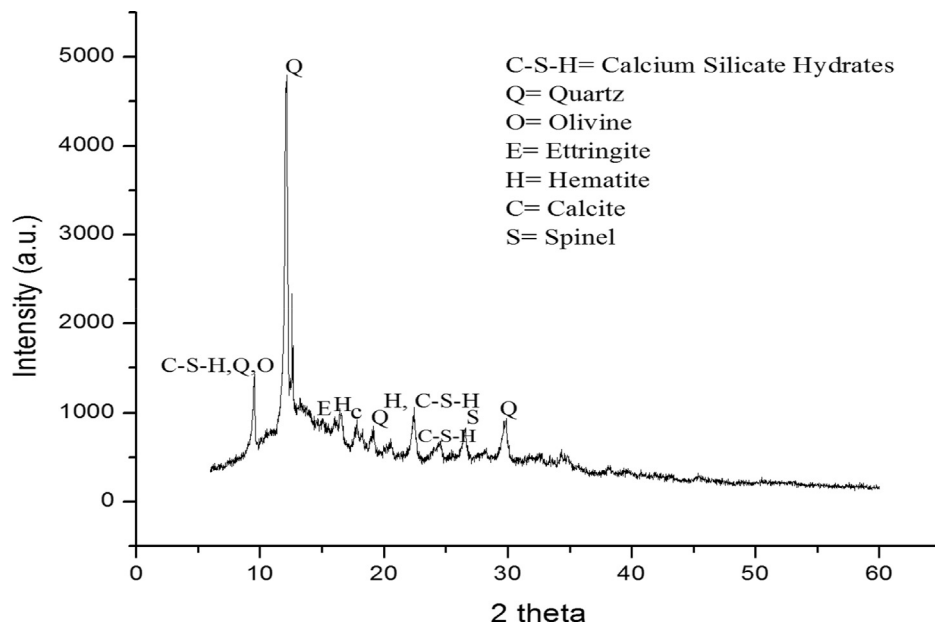


Fig. 14. XRD image of Geopolymer mix with FS 0%.

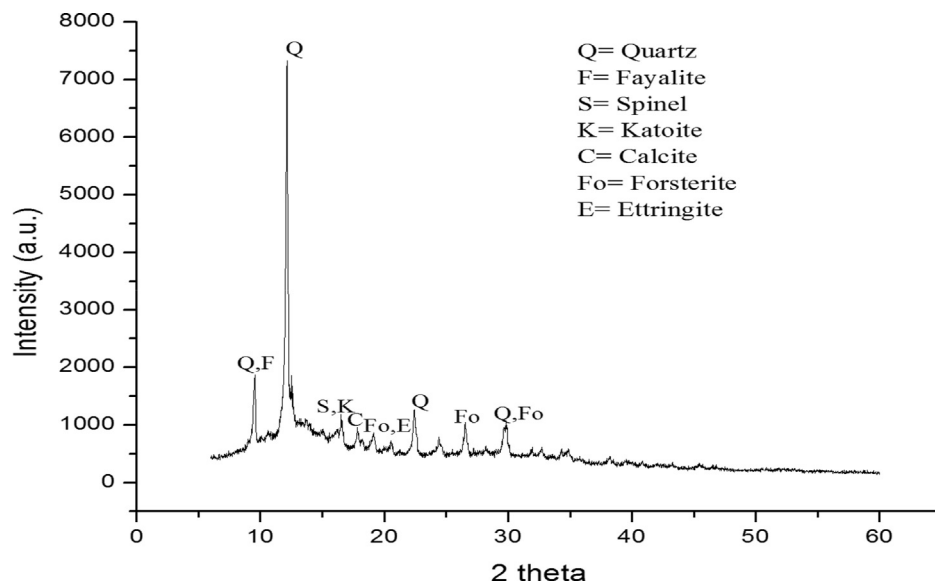


Fig. 15. XRD image of Geopolymer mix with FS 10%.

This band was noticed when the amount of FS is more for the reaction and the shifting of this band occurs towards higher frequency. This could be due to the geopolymerization which was changed the Si/Al ratio. This is the main reason behind the structural alteration of the Si/Al network [54,55]. Maximum absorption was obtained at  $998.85\text{ cm}^{-1}$  with respect to 90.3% transmittance. Another band  $693.86\text{ cm}^{-1}$  was subjected to medium absorption corresponds to the 94.4% transmittance. Very weak absorbance was noticed at  $1982.2\text{ cm}^{-1}$ ,  $2021.5\text{ cm}^{-1}$ ,  $2150.3\text{ cm}^{-1}$  and  $2193.42\text{ cm}^{-1}$  corresponding to 99.14%, 99.5%, 99.24% and 99.37% transmittance. A weak stretching vibration of C–C triple bonds was assigned to  $2150\text{ cm}^{-1}$  band. Strong stretching vibration of Si–O–Si and Si–O–Al bonds was assigned to  $693\text{ cm}^{-1}$  band [56]. This could be due to the presence of ferrochrome slag in GPC [25].

It is observed from the above four FTIR spectra as the percentage of FS increased from FS0 to FS30, strong absorption is noticed

in the region  $990\text{--}1000\text{ cm}^{-1}$ . Like that, transmittance is also increased with respect to increase in FS percentage in the geopolymer concrete mix.

#### 4.6. XRD analysis

XRD images of geopolymer mixes with different percentage of FS are shown in Figs. 14–17. Fig. 14 shows XRD graph of controlled mix. It was observed that maximum intensity of quartz mineral was found to be 4700. Olivine ( $\text{Mg, Fe}_2\text{SiO}_4$ ) is identified in the control mix. Its compositions are expressed as different percentage of fayalite ( $\text{Fe}_2\text{SiO}_4$ ) and forsterite ( $\text{Mg}_2\text{SiO}_4$ ). But peak of this two minerals are separately observed in the XRD analysis of FS10 mix. Fayalite ( $\text{Fe}_2\text{SiO}_4$ ) is observed at peak nearly 2000 and also called as crystalite. It is much compatible and stable with quartz even at low temperature. Presence of forsterite ( $\text{Mg}_2\text{SiO}_4$ ) is almost very low

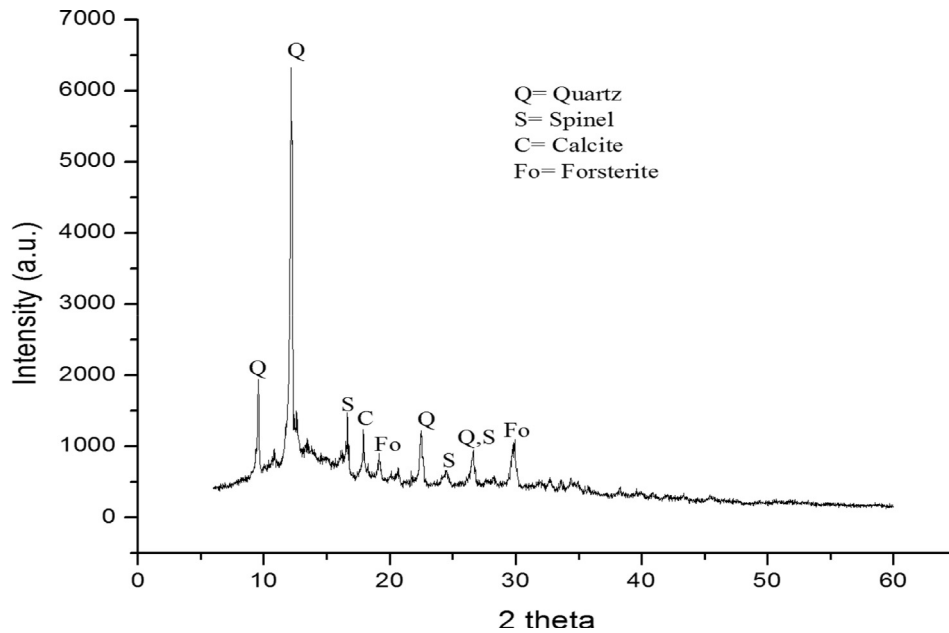


Fig. 16. XRD image of Geopolymer mix with FS 20%.

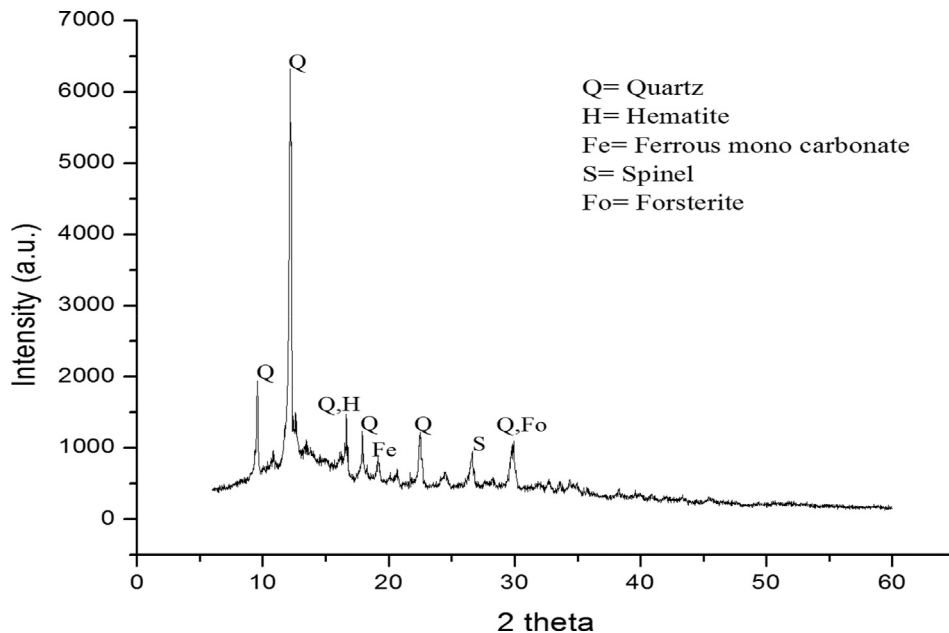


Fig. 17. XRD image of Geopolymer mix with FS 30%.

nearly about 800–1100. Spinel phases are observed in all the XRD analysis figures. Some amount of C-S-H (Calcium Silicate Hydrates) gel is observed in control mix. Hematite, calcite, ettringite, katoite and ferrous mono carbonates are identified in the XRD analysis of GPC mix with different percentage of FS. There are different crystalline phases available such as spinel, forsterite and quartz etc. Highest peak was noticed due to quartz. After geopolymerization, intensity of crystalline peak was reduced. Finally, it was converted to hardened amorphous or semi-crystalline phase. This structural change is identified by FTIR analysis in which Si–O–Si and Al–O–Al bond was shifted [25]. Fig. 15 shows the XRD graph of geopolymer mix with 10% FS. Peaks were due to the presence of quartz ( $\text{SiO}_2$ ), spinel ( $\text{MgAl}_2\text{O}_4$ ), forsterite ( $\text{Mg}_2\text{SiO}_4$ ) and calcite etc [53]. Broad peaks were seen in the region  $9-32^\circ 2\theta$  [26]. It is observed that consumption of quartz was more in Fig. 15 which is more than control GPC. This may be the reason for strength gain. Peak of quartz mineral showed the maximum availability of free silica in GPC mixes. Maximum peak of quartz is observed in the mix FS 10. It is nearly around 7300. This intensity is nearly about 2000 higher than that of FS0. In the Figs. 16 and 17, FS 20 and FS 30 mixes show maximum peak of  $\text{SiO}_2$  is noticed nearly 6400. It was noticed from these figures that controlled mix has lower intensity of the mineral phases than other three figures. This could be due to more strength of FS than NCA, which require higher intensity to determine the mineral phases of the material. All the crystalline phases lost their and transformed into poorly crystalline phases in the mix FS10, FS20 and FS30 due to the use of FS. But more crystalline phases are remaining un-reacted. Some of the crystalline phases are available in the fly ash. Quartz is the major crystalline phase which is non-activated part. Similarly, spinel and forsterite are the main remnant phase. The carbonate phase of calcite shows the weak peaks [25].

#### 4.7. SEM analysis

SEM test was conducted to study the micro structural characteristics of GPC samples. The samples were used for micro structure analysis was taken from the surface of the GPC cubes. Figs. 18 (a), (b) and (c) showed the SEM images of the GPC samples G2, G4, G6 which corresponds to the solution to binder ratio 0.4, 0.5 and 0.6 respectively. These figures showed the effectiveness of the alkaline activation process. It indicates that the geopolymerization reaction was occurred with the addition of alkaline activators of varying concentrations. Higher degree of reaction causes higher CS achievement [57]. Also Fig. 19 (a), (b) and (c) corresponds to EDX images of the above mentioned samples. It is observed that SEM image of G4 sample is very compacted and

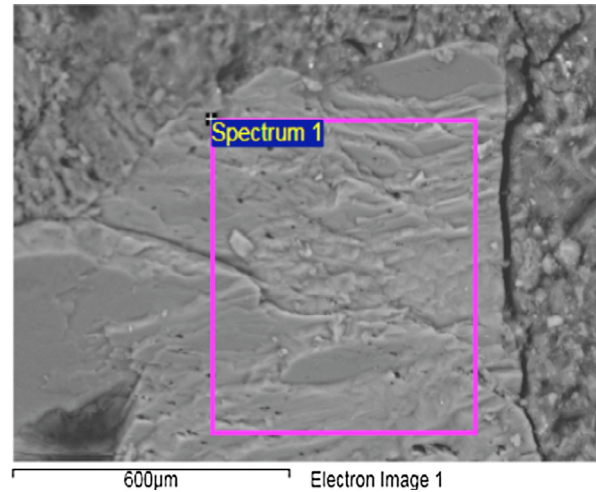


Fig. 18b. SEM image of G<sub>4</sub> sample.

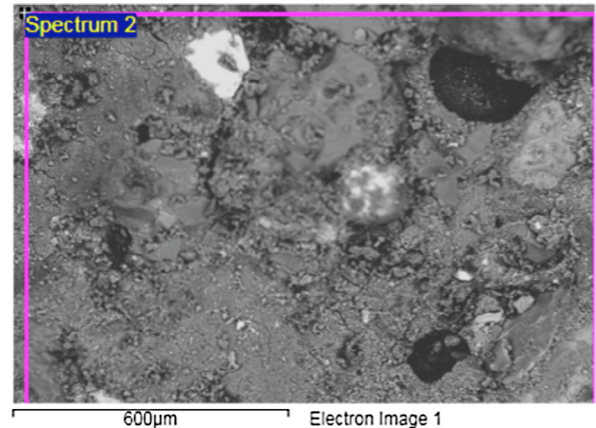


Fig. 18c. SEM image of G<sub>6</sub> sample.

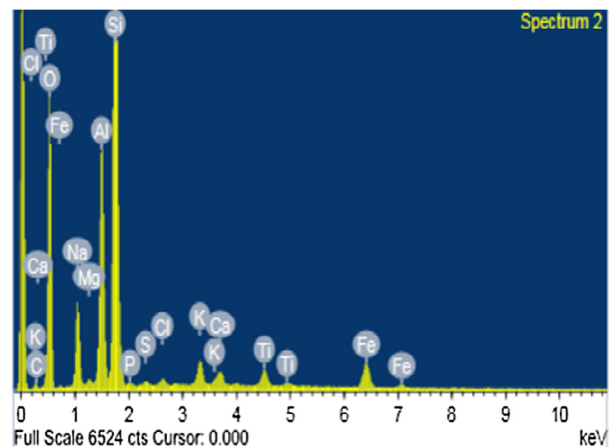


Fig. 19a. EDX of G<sub>2</sub> sample.

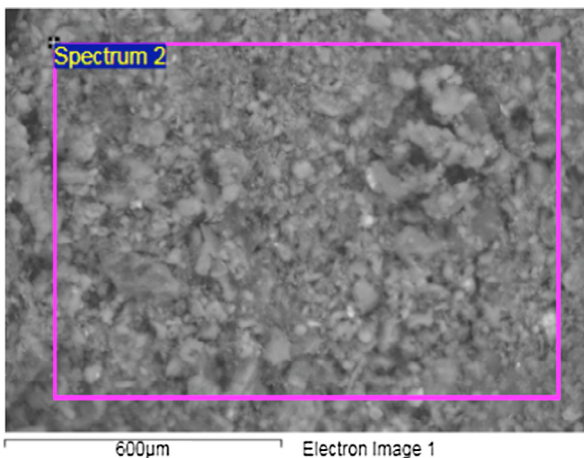


Fig. 18a. SEM image of G<sub>2</sub> sample.

dense, which shows that increase in the solution to binder ratio increases the compactness. That image seemed to be one plane surface and no unreacted particles are available. Increasing solution to binder ratio means alkaline solution quantity is increasing at constant fly ash quantity. Further, more percentage of SS solution is available in the total amount of alkaline solutions. Hence,

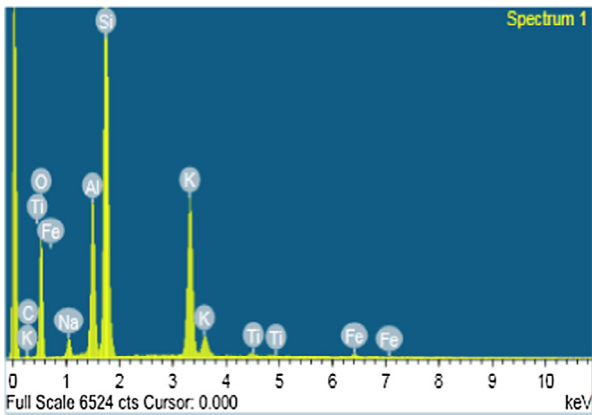


Fig. 19b. EDX of G<sub>4</sub> sample.

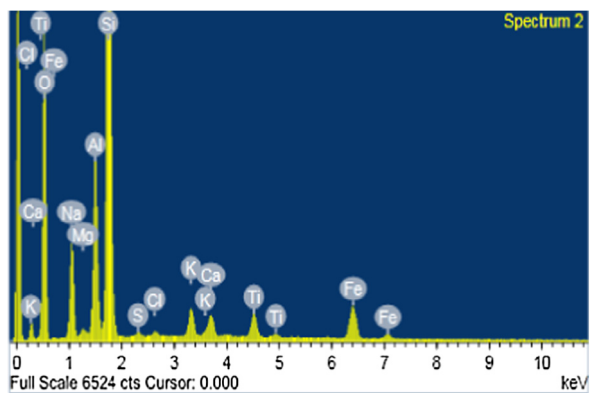


Fig. 19c. EDX of G<sub>6</sub> sample.

SS quantity increases with the increase in the ratio. This could be the reason for strength development of G<sub>4</sub> sample than G<sub>2</sub> sample. It is noticed from the SEM image of G<sub>2</sub> sample that it is less dense and compacted than other two specimens. G<sub>6</sub> sample image is also more compacted and denser image than other SEM images. This might be the reason behind the strength development than other geopolymer mixes. Strength was achieved due to the geopolymerization reaction of Al–Si with alkaline activators [58].

Fig. 20(a), (b), (c) and (d) show the SEM images of hardened GPC mixes with different percentage of FS i.e. 10%, 20%, 30% and 0% in



Fig. 20a. SEM image of FS10 sample.



Fig. 20b. SEM image of FS20 sample.

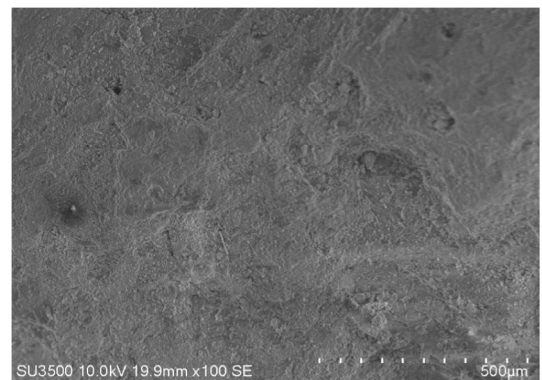


Fig. 20c. SEM image of FS30 sample.

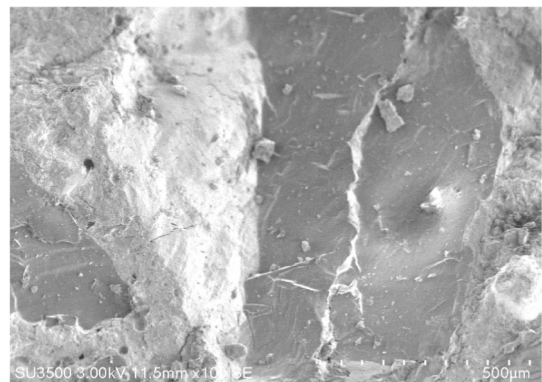


Fig. 20d. SEM image of FS0 sample.

place of natural coarse aggregate. It is observed from the Fig. (a) and (b) shows that aluminosilicate matrix in different shapes are occurred on the surface. This could be the reason for the development of CS of GPC samples. Aluminosilicate gel offers significant bearing resistance against the compressive load on the GPC samples. Fig. (d) shows the microstructure of FS0. Continuous matrices are formed in controlled GPC with less porous and homogeneous structure as noticed in Fig. (c). Some micro cracks created due to evaporation of water during curing are also observed.

## 5. Conclusions

This experimental study has presented an innovative research work by producing geopolymers using 100% fly ash as a binder and partial replacement of ferrochrome slag with natural coarse aggregate. The mechanical properties of FSGPC have been reported for different percentages of replacement of FS with NCA. Further, EDX, SEM, XRD and FT-IR analysis are also presented. The properties and interrelation between CS and STS of fly ash GPC with maximum percentage of FS has been studied. The following summary statements are drawn from the above-mentioned results: -

1. The slump value of fly ash GPC increases with increasing percentage of ferrochrome slag and solution to binder ratio.
2. A higher percentage of ferrochrome slag is used as partial replacement of natural coarse aggregate in fly ash GPC. Higher compressive strength is achieved in FSGPC compared to the controlled GPC. Strength is found to be 49 MPa comparable with high strength concrete of 40 MPa. This implies FSGPC has ability to produce high strength concrete and it can replace cement concrete. Compressive strength of FS 30 with solution to binder ratio 0.6 is found to be maximum among all the mixes with varying binder ratio. The optimum strength may be due to the maximum geopolymerization of the activator solution.
3. The other mechanical properties such as split tensile strength and flexural strength of the FSGPC increase with the increase in percentage of FS up to 30% in comparison to the corresponding value of controlled GPC. But the strengths decrease at FS content 35% and 40%.
4. A reliable relationship was established between CS and STS of fly ash GPC with FSGPC with 30% replacement of FS with NCA. Further, a new equation was proposed between CS and flexural strength is found out by regression analysis.
5. The SEM-EDS analysis facilitated to demonstrate the compactness and geopolymerization of the structure of GPC activated with varying solution to binder ratio and varying percentage of FS used. Non-reacted particles could be observed from the images.
6. XRD test was carried out to analyze the crystallinity of the material structure. The reaction products were generated by the alkali activation process in which aluminosilicate substances were amorphous in structure. From the above analysis, crystalline phases are identified and their effects are reported.
7. Indirect analysis was done through degree of geopolymerization in FT-IR analysis. This test was conducted to observe the reason behind deviation in the mechanical properties of GPC.

## Declaration of Competing Interest

There are no conflicts between the corresponding author and co-author regarding this manuscript submission. This is the combined effort of both.

## References

- [1] M. Nadeem, A.D. Pofale, Utilization of industrial waste slag as aggregate in concrete applications by adopting Taguchi's approach for optimization, *Open J. Civ. Eng.* 2 (2012) 96–105.
- [2] A. Islam, U.J. Alengaram, M.Z. Jumaat, I.I. Bashar, The development of compressive strength of ground granulated blastfurnace slag-palm oil fuel ash-fly ash based geopolymer mortar, *Mater. Des.* 56 (2014) 833–841.
- [3] C.N. Harman, Innovations in ferroalloys technology in India, *INFACON XI* (2007) 25–37.
- [4] C.R. Panda, K.K. Mishra, K.C. Panda, B.D. Nayak, B.B. Nayak, Environmental and technical assessment of ferrochrome slag as concrete aggregate material, *Constr. Build. Mater.* 49 (2013) 262–271.
- [5] S.K. Slanic, The influence of fly ash fineness on the strength of concrete, *Cem. Concr. Res.* 21 (1991) 285–296.
- [6] V. Sata, C. Jaturapitakkul, C. Rattanashotinunt, Compressive strength and heat evolution of concretes containing palm oil fuel ash, *J. Mater. Civ. Eng.* 22 (2010) 1033–1038.
- [7] P. Chindaprasirt, S. Homwuttiwong, V. Sirivivatnanon, Influence of fly ash fineness on strength, drying shrinkage and sulfate resistance of blended cement mortar, *Cem. Concr. Res.* 34 (2004) 1087–1092.
- [8] J. Davidovits, Geopolymer: inorganic polymeric new materials, *J. Therm. Anal.* 37 (1991) 1633–1656.
- [9] J. Temuujin, A. Minjigmaa, M. Lee, N. Chen-Tan, A. Van Riessen, Characteristic of class F fly ash geopolymer pastes immersed in acid and alkaline solutions, *Cem. Concr. Compos.* 33 (2011) 1086–1091.
- [10] V. Sata, A. Sathonsaowaphak, P. Chindaprasirt, Resistance of lignite bottom ash geopolymer mortar to sulfate and sulfuric acid attack, *Cem. Concr. Compos.* 34 (2012) 700–708.
- [11] P. Chindaprasirt, T. Chareerat, V. Sirivivatnanon, Workability and strength of coarse high calcium fly ash geopolymer, *Cem. Concr. Compos.* 29 (2007) 224–229.
- [12] J. Zelic, Properties of concrete pavements prepared with ferrochromium slag as concrete aggregate, *Cem. Concr. Res.* 35 (2005) 2340–2349.
- [13] C.S. Poon, Z.H. Shui, L. Lam, Effect of microstructure of ITZ on compressive strength of concrete prepared with recycled aggregates, *Constr. Build. Mater.* 18 (2004) 461–468.
- [14] M. Etxeberria, A. Mari, E. Vazquez, Recycled aggregate concrete as structural material, *Mater. Struct.* 40 (2007) 529–541.
- [15] M. Limbachiya, M.S. Meddah, Y. Ouchagour, Use of recycled concrete aggregate in fly-ash concrete, *Constr. Build. Mater.* 27 (2012) 439–449.
- [16] R.K. Majhi, A.N. Nayak, B.B. Mukharjee, Development of sustainable concrete using recycled coarse aggregate and ground granulated blast furnace slag, *Constr. Build. Mater.* 159 (2018) 417–430.
- [17] W. Tangchirapat, R. Buranasing, C. Jaturapitakkul, P. Chindaprasirt, Influence of rice husk-bark ash on mechanical properties of concrete containing high amount of recycled aggregates, *Constr. Build. Mater.* 22 (2008) 1812–1819.
- [18] V. Sata, A. Wongsu, P. Chindaprasirt, Properties of pervious geopolymer concrete using recycled aggregates, *Constr. Build. Mater.* 42 (2013) 33–39.
- [19] P. Posi, C. Teerachanwit, C. Tanutong, S. Limkamoltip, S. Lertnimoolchai, V. Sata, P. Chindaprasirt, Lightweight geopolymer concrete containing aggregate from recycle lightweight block, *Mater. Des.* 52 (2013) 580–586.
- [20] T.T. Teing, B.B.K. Huat, S.K. Shukla, V. Anggraini, H. Nahazanan, Effects of Alkali-Activated Waste Binder in Soil Stabilization, *Int. J.* 17 (2019) 82–89.
- [21] Y. Lee, J.J. Bang, S. Kang, Study on a nano-microstructure and properties of geopolymer by recycling integrated gasification combined cycle coal ash slag, *J. Nanosci. Nanotechnol.* 19 (2019) 2193–2197.
- [22] C. Yan, L. Guo, D. Ren, P. Duan, Novel composites based on geopolymer for removal of Pb (II), *Mater. Lett.* 239 (2019) 192–195.
- [23] A. Mehta, R. Siddique, Sustainable geopolymer concrete using ground granulated blast furnace slag and rice husk ash: strength and permeability properties, *J. Clean. Prod.* 205 (2018) 49–57.
- [24] S. Pilehvar, V.D. Cao, A.M. Szczotok, M. Carmona, L. Valentini, M. Lanzón, R. Pamies, A.-L. Kjøniksen, Physical and mechanical properties of fly ash and slag geopolymer concrete containing different types of micro-encapsulated phase change materials, *Constr. Build. Mater.* 173 (2018) 28–39.
- [25] S.K. Nath, Geopolymerization behavior of ferrochrome slag and fly ash blends, *Constr. Build. Mater.* 181 (2018) 487–494.
- [26] M.B. Karakoç, I. Türkmen, M.M. Maraş, F. Kantarcı, R. Demirboğa, M.U. Toprak, Mechanical properties and setting time of ferrochrome slag based geopolymer paste and mortar, *Constr. Build. Mater.* 72 (2014) 283–292.
- [27] M.K. Dash, S.K. Patro, Performance assessment of ferrochrome slag as partial replacement of fine aggregate in concrete, *Eur. J. Environ. Civ. Eng.* (2018) 1–20.
- [28] A.W. Abhijit, Y.M. Nigade, Technical Assessment on Performance of Partial Replacement of Coarse Aggregate by Steel Slag in Concrete, *Int. J. of Eng. Technol.* 30 (2016) 37–41.
- [29] IS: 3812 Indian Standard Specification Pulverised fuel ash specification (part-1), Bureau of Indian Standards, New Delhi, 1970.
- [30] IS: 3831 Indian Standard Specification for Coarse and Fine Aggregate from Natural Sources, Bureau of Indian Standards, New Delhi, 1970.
- [31] M. Albitar, P. Visintin, M.S.M. Ali, M. Drechsler, Assessing behaviour of fresh and hardened geopolymer concrete mixed with class-F fly ash, *KSCE J. Civ. Eng.* 19 (2015) 1445–1455.
- [32] IS: 2386 Indian Standard Specification, Methods of test for aggregates for concrete: Part 1, Particle size and shape, Bureau of Indian Standards, New Delhi, 1963.
- [33] IS: 2386 Indian Standard Specification, Methods of Test for Aggregates for Concrete: Part 3, Specific Gravity, Density, Voids, Absorption and Bulking, Bureau of Indian Standards, New Delhi, 1963 [Reaffirmed in 2002].
- [34] IS: 2386 Indian Standard Specification, Methods of Test for Aggregates for Concrete: Part 4, Mechanical Properties, Bureau of Indian Standards, New Delhi, 1963 [Reaffirmed in 2002].
- [35] M. Ozturk, M.B. Bankir, O.S. Bolukbasi, U.K. Sevim, Alkali activation of electric arc furnace slag: Mechanical properties and micro analyzes, *J. Build. Eng.* 21 (2019) 97–105.
- [36] IS: 5816 Splitting Tensile Strength of Concrete – Method of Test, Bureau of Indian Standards, New Delhi, India, 1999.
- [37] IS: 516 Indian Standard Methods of Tests for Strength Concrete, Bureau of Indian Standards, New Delhi, 1959.

- [38] R.H. Haddad, O. Alshbuol, Production of geopolymer concrete using natural pozzolan: A parametric study, *Constr. Build. Mater.* 114 (2016) 699–707.
- [39] F.N. Okoye, J. Durgaprasad, N.B. Singh, Mechanical properties of alkali activated flyash/Kaolin based geopolymer concrete, *Constr. Build. Mater.* 98 (2015) 685–691.
- [40] ASTM C642-13 Standard Test Method for Density, Absorption, and Voids in Hardened Concrete, ASTM International, West Conshohocken, 2013.
- [41] J.K. Prusty, S.K. Patro, T. Mohanty, Structural behaviour of reinforced concrete beams made with ferrochrome slag as coarse aggregate, *KSCE J. Civ. Eng.* 22 (2018) 696–707.
- [42] P.K. Acharya, S.K. Patro, Utilization of ferrochrome wastes such as ferrochrome ash and ferrochrome slag in concrete manufacturing, *Waste Manag. Res.* 34 (2016) 764–774.
- [43] A.A. Aliabdo, A.E.M.A. Elmoaty, H.A. Salem, Effect of water addition, plasticizer and alkaline solution constitution on fly ash based geopolymer concrete performance, *Constr. Build. Mater.* 121 (2016) 694–703.
- [44] S. Jena, R. Panigrahi, P. Sahu, Effect of silica fume on the properties of fly ash geopolymer concrete, *Sustain. Constr. Build. Mater.* Springer (2019) 145–153.
- [45] R. Sathia, K.G. Babu, M. Santhanam, Durability study of low calcium fly ash geopolymer concrete, *Proceedings of the 3rd ACF International Conference-ACF/VCA*, 2008.
- [46] M.F.M. Zain, H.B. Mahmud, A. Ilham, M. Faizal, Prediction of splitting tensile strength of high-performance concrete, *Cem. Concr. Res.* 32 (2002) 1251–1258.
- [47] ACI 363R-92 State-of-the-art Report on High-strength CONCRETE ACI committee report 363, American Concrete Institute, Detroit, 1992, pp. 363R1–363R55.
- [48] Committee Euro-International du Beton (CEB-FIP). CEB-FIP model code 1990, Thomas Telford, London; 1993.
- [49] N.J. Gardner, S.M. Poon, Time and temperature effects on tensile, bond, and compressive strengths, *J. Proc.* (1976) 405–409.
- [50] G.S. Ryu, Y.B. Lee, K.T. Koh, Y.S. Chung, The mechanical properties of fly ash-based geopolymer concrete with alkaline activators, *Constr. Build. Mater.* 47 (2013) 409–418.
- [51] A.C.I. Committee, A.C. Institute, I.O. for Standardization, Building Code Requirements for Structural Concrete (ACI 318-08) and Commentary, American Concrete Institute, 2008.
- [52] M. Sofi, J.S.J. Van Deventer, P.A. Mendis, G.C. Lukey, Engineering properties of inorganic polymer concretes (IPCs), *Cem. Concr. Res.* 37 (2007) 251–257.
- [53] T. Bakharev, Durability of geopolymer materials in sodium and magnesium sulfate solutions, *Cem. Concr. Res.* 35 (2005) 1233–1246.
- [54] S.K. Nath, S. Kumar, Reaction kinetics, microstructure and strength behavior of alkali activated silico-manganese (SiMn) slag – fly ash blends, *Constr. Build. Mater.* 147 (2017) 371–379.
- [55] X. Gao, Q.L. Yu, H.J.H. Brouwers, Reaction kinetics, gel character and strength of ambient temperature cured alkali activated slag-fly ash blends, *Constr. Build. Mater.* 80 (2015) 105–115.
- [56] A.K. Panda, B.G. Mishra, D.K. Mishra, R.K. Singh, Effect of sulphuric acid treatment on the physico-chemical characteristics of kaolin clay, *Colloids Surf. A Physicochem. Eng. Asp.* 363 (2010) 98–104.
- [57] J. Davidovits, D.C. Comrie, J.H. Paterson, D.J. Ritcey, Geopolymeric concretes for environmental protection, *Concr. Int.* 12 (1990) 30–40.
- [58] J. Davidovits, *Geopolymer Chemistry and Applications*, Geopolymer Institute, 2008.